Dalmau-Borrás, A.; Roda Buch, A.; Rovira, A.; Navarro-Laboulais, J.; Igual Muñoz, AN. (2019). Chemo-mechanical effects on the tribocorrosion behavior of titanium/ceramic dental implant pairs in artificial saliva. Wear. 426-427:162-170. https://doi.org/10.1016/j.wear.2018.12.052

Chemo-mechanical effects on the tribocorrosion behavior of titanium/ceramic dental implant pairs in artificial saliva

A. Dalmau Borrás[1], A. Roda Buch[2], A. Rovira[3], J. Navarro-Laboulais[1], A. Igual-Muñoz[2]

[1] ISIRYM, Universitat Politecnica de Valencia. Camino de Vera s/n, 46022 Valencia, SPAIN

[2] TIC, Ecole Polytechnique Federale de Lausanne. CH-1015 Lausanne, SWITZERLAND

[3] CIIM, Universitat Politecnica de Valencia. Camino de Vera s/n, 46022 Valencia, SPAIN

Abstract

In this paper, the degradation mechanisms of the ceramic and the metal in Titanium/Zirconia pairs for biomedical applications were analysed. To do that, an experimental set-up with well-controlled mechanical and chemical conditions was used based on a unidirectional ball-on-disk tribometer coupled to a potentiostat. Tribocorrosion tests were carried out in artificial saliva at different applied potentials, this is, different chemical conditions of the surface. Wear damage of the titanium/zirconia pair was influenced by the properties and the behavior of wear debris in the contact. Under passive conditions metallic and oxidized titanium particles (formed by the cyclic removal of the passive film and subsequent repassivation) were smeared and mechanically mixed within the contact forming compacted wear debris through which the loading was carried out. Properties and amount of oxidized titanium lead to low wear at low passive conditions (OCP) and higher wear at high passive conditions. Zirconia did not suffer any damage under all the studied conditions and oxidized titanium was transferred to the ball at anodic applied potentials.

Keywords: tribocorrosion, titanium, ceramic, dental

1. Introduction

Chemical and mechanical interaction in tribological contacts lead to a tribocorrosion material degradation typically present in applications such as biomedical, power plants, oil and gas or manufacturing [1]. In dental applications, metal/ceramic contacts are commonly found in the implant design immersed in a corrosive environment, the saliva, thus constituting a tribocorrosion system. During the service life of those implants, they are subjected to different mechanical conditions (i.e. cyclic loading) and chemical ones (i.e. pH or electrode potential changes).

It has been widely reported the importance of studying the effect of the wear and corrosion together, the tribocorrosion degradation. The importance of these phenomena is confirmed by the increasing number of publications in the field [2]. Over the last decades, different studies have been carried out regarding tribocorrosion of titanium and its alloys in order to understand the involved phenomena that take place inside the human body. Several review papers have been published trying to rationalize the degradation behavior of titanium alloys. Long and Rack [3] published a first review on the physical and the mechanical properties of titanium alloys used in artificial joint replacement prostheses and its influence on wear behavior. They highlighted the need for the development of new beta-alloys with a reduced elastic modulus, closer to the one measured in the bone to avoid the stress-shielding effect, and the understanding of the involved wear mechanisms. In 2015, Souza et al. [4] published a literature review concerning the wear, corrosion and their interactions on titanium in oral environment. They reported the bio-tribocorrosion as the governing mechanism of the degradation of titanium in the oral cavity, thus the importance of controlling the mechanical conditions in the dental implants but also the complex biological environment of the saliva for understanding the final behavior of titanium. More recently, Revathi et al. [5] reviewed the degradation mechanism of titanium and surface treatments to improve the performance and the service life of dental implants. The release of metal ions and wear products caused by tribocorrosion were reported to result in the activation of a cascade of immunologic response which finally may result in the failure of the dental implant. Fretting corrosion that can occur at the interface between the implant and alveolar bone during occlusal movements was also reported as a relevant degradation mechanism controlled by the material properties, chemical composition of the environment and mechanical conditions in the contact. In the different tribocorrosion studies reported in [5], ceramic alumina was used as counterpart and wear coefficients in the order of 10^{-4} mm^3/Nm were reported.

Although all tribocorrosion studies were carried using different counterparts (Al_2O_3, Si_3N_4, steel or UHMWPE), most dental implant systems consist in dental prosthesis, usually made by zirconia (ZrO_2), fixed with an abutment and an implant made by titanium [4]. Zirconia was considered to be a better alternative for alumina as alumina is highly brittle [6]. Recently, Sikora et al. [7] studied the wear and corrosion interactions at the titanium/zirconia interface for dental applications. They quantified the material loss during tribocorrosion of pure titanium and roxolid alloy (Ti-13Zr) rubbed against ZrO_2 and the corresponding self-matted contacts. They also observed that the titanium rubbed against zirconia presented the lowest wear volume. However, the reasons justifying this superior behavior of Ti-ZrO_2 contact could not be given. It was then highlighted that understanding the physicochemical phenomena taking place at

the interface of a metal/ceramic system is necessary for the development of new alloys and surface modifications for biomedical applications.

Klotz et al. [8] also studied the effect of the implant material abutment (titanium or zirconia) in the wear of titanium implants and they observed that the implants with the zirconia abutments showed a higher initial wear rate and also higher total wear than the implants with the titanium abutments after cyclic loading tests. The amount of titanium transfer on the zirconia abutment increased with the number of loading cycles but appeared to be self-limiting. These observations lead to hypothesize a change in wear mechanisms occurring as the loading cycles increase. Clearly, further investigations are needed to better understand the interaction between metal/ceramic contacts in dental implant systems.

In order to mimic the dental system, recently Mendes et al. [9] established that the sphere-plane system (ball-on-disk configuration) is a method that can be used to evaluate and quantify the wear of the titanium of dental implants. They compared this system with other methods that use real implants and they conclude that the use of the tribometer in a ball-on-disk configuration is the much simpler and less expensive set-up.

In this work, the tribocorrosion behavior of pure titanium rubbed against a ZrO_2 ceramic counterpart will be characterized. For that purpose, ball-on-disk tribocorrosion tests have been carried out in the Ti/ZrO_2 pair under different electrochemical conditions in artificial saliva.

2. Experimental

2.1. Materials

Titanium grade 4 has been used in this study from the *Straumann* commercial company. Specimens had geometry of disks of 15 mm in diameter and 1 mm in thickness. These samples were tested as received: SLA® surface [10] and sterilized. They have an average roughness of R_a = 2.9 µm. Table 1 shows the chemical composition of the sample.

Table 1. Chemical composition of the Ti (4) sample in wt.%.

	Zr	O	Fe	N	C	H	Ti
Ti (4)	-	0.18 - 0.24	≤ 0.050	≤ 0.02	≤ 0.05	≤ 0.005	Bal.

The counterpart used in the tribocorrosion test was zirconia (Zr_2O + 3 M Y_2O_3) ball of 6 mm of diameter obtained from Aparicio S.L. (Spain). They were finished according to the ISO 3290 standard, with a degree of precision G28 (R_a = 0.05 µm).

2.2. Mechanical characterization

Microstructure of the Ti sample has been obtained using Kroll's reagent (3 ml HF, 6 ml HNO_3, 100 ml H_2O). Microstructure of the ZrO_2 ball was revealed by heat treatment: 1200 ºC during 30 min.

A microdurometer Duramin from Struers was used to measure the microhardness values of the samples. For that purpose, a load of 0.2 kg was applied with a Vickers indenter during 30 s ($HV_{0.2}$).

The elastic modulus and the Poisson's ratio were obtained from the datasheet of the suppliers of the studied materials.

2.3. Electrochemical equipment and solution

A typical three-electrode cell connected with an Autolab 302N was used to carry out the electrochemical measurements. A Ag/AgCl (3M) was used as reference electrode, a Pt wire as counter electrode and the Ti sample as working electrode. All potentials are given to respect the reference electrode.

Before running any experiment, samples were kept at -1.5 V during 300 s. Cathodic polarization curves were carried out starting from the open circuit potential (OCP) value and cathodically decreasing the potential until -1.5 V. Sequentially, an anodic scan was carried out by increasing the applied potential in the anodic direction until 2 V. The scan rate was 1 mV/s for all polarization curves.

An artificial saliva (AS) with similar properties to those of the real saliva at a temperature of 37ºC has been used as the electrolyte of the electrochemical and tribocorrosion tests. Table 2 shows the chemical composition of the AS.

Table 2. Chemical composition of the AS.

Compound	Concentration (g/L)
NaCl	0.40
KCl	0.40
$CaCl_2$	0.60
Na_2HPO_4	1.46
Urea	1.00

2.4. Tribocorrosion tests

2.4.1. Experimental set-up

A tribometer with a pin-on-disk configuration has been used for carrying out the tribocorrosion tests (Figure 1). A normal force of F_N = 5 N has been applied to the counterpart. The initial maximum and average contact pressure exerted by the counterpart on the sample were 647 MPa and 584 MPa, respectively. The wear track radius was r_{wt} = 1 mm and the sliding velocity v = 6.28 mm/s (ω = 60 rpm).

An electrochemical cell connected to a potentiostat was integrated in the tribometer in order to register the potential and the current evolution with time during the tribocorrosion tests. This configuration was the same as mentioned in section 2.3.

Tribocorrosion tests were carried out under three different electrochemical conditions: (1) at OCP, (2) at applied cathodic potential of -1.5 V and (3) at applied anodic potential of 1 V. Before running any test, samples were kept at -1.5 V during 300 s. Then, the OCP was measured or the specific potential was applied while recording the response in current for 1800 s. After the stabilization period, the sliding started under the selected electrochemical conditions and lasted for 3600 s (3600 cycles). Finally, the system was kept at the applied potentials for 300 s.

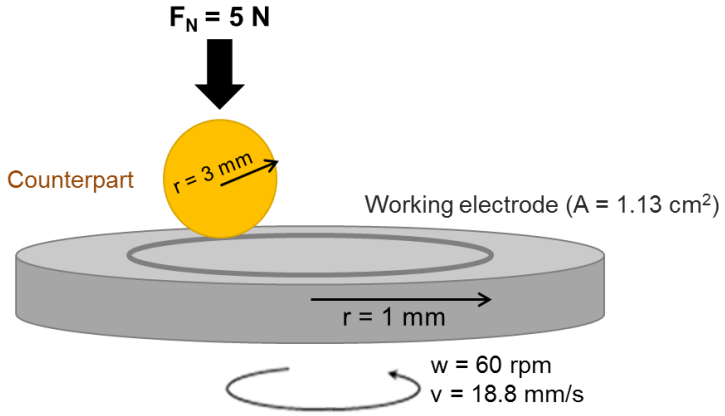

Figure 1. Experimental set-up for the tribocorrosion tests.

2.4.2. Wear characterization

After the tribocorrosion tests, all samples were analysed using an optical microscope coupled with a confocal laser. Material lost after tribocorrosion test was carried out by confocal microscopy. The total wear volume (V_T) was quantified from five profiles of the wear track, obtaining an average transversal wear area and multiplying it by the length of one cycle (6.28 mm).

Wear morphology of the wear track of the Ti samples and the ceramic balls were analyzed by means of a Field Emission Electronic Scanning Microscope (FESEM) Zeiss Auriga Compact. The voltage was 3 kV in case of the Ti samples and 1 kV in case of the ceramic balls.

Cross-sections of the wear track have been made by means of a Focus Ion Beam (FIB) system. Trapezoid trench of 10 x 10 µm and 10 µm depth was cut by the gallium ion beam using an intensity of 500 pA. When needed, a thin layer of platinum was deposited on the surface before cutting. The images were taken on the worn surfaces perpendicular to the sliding direction by the FESEM.

3. Results

3.1. Microstructural and mechanical characterization

Table 3 summarizes the values of the hardness, Young's modulus and Poisson's ratio of the studied materials.

Table 3. Physical and mechanical properties of the different studied materials.

	Hardness H (GPa)	Young's Modulus E (GPa)	Poisson's Ratio ν -
Ti (4)	2.7	105	0.37
Zr_2O	13.2	213	0.25

The microstructure of the titanium sample is shown in Figure 2. The studied titanium presents a fully equiaxed microstructure with the grain size ranging from 5 to 30 µm. SEM images of the surface and the microstructure of the ZrO_2 ball are shown in Figure 3. The zirconia ball presents a compact microstructure, with grain size varying from 100 to 500 nm.

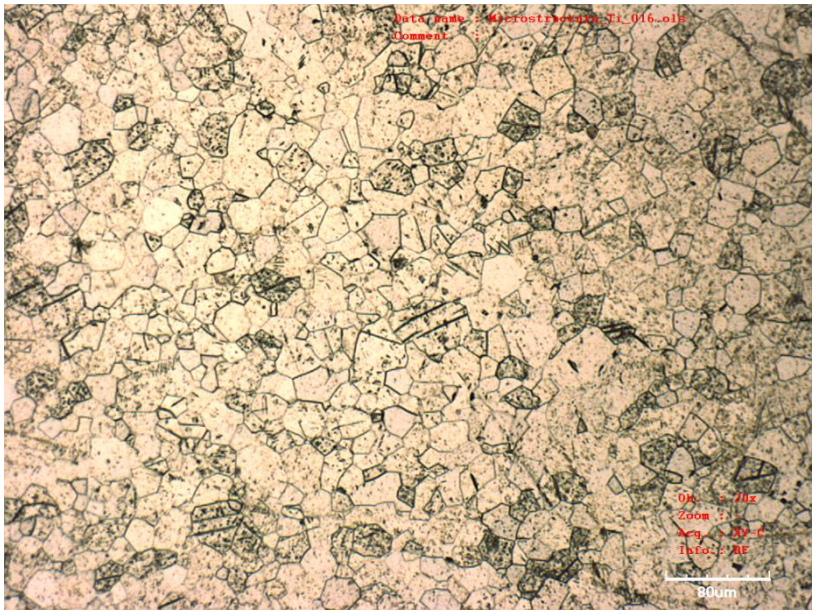

Figure 2. Optical image of the microstructure of the studied Ti sample.

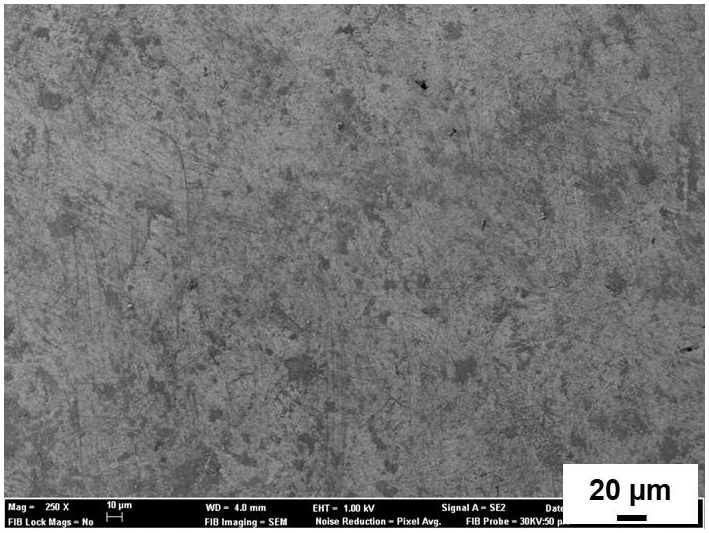

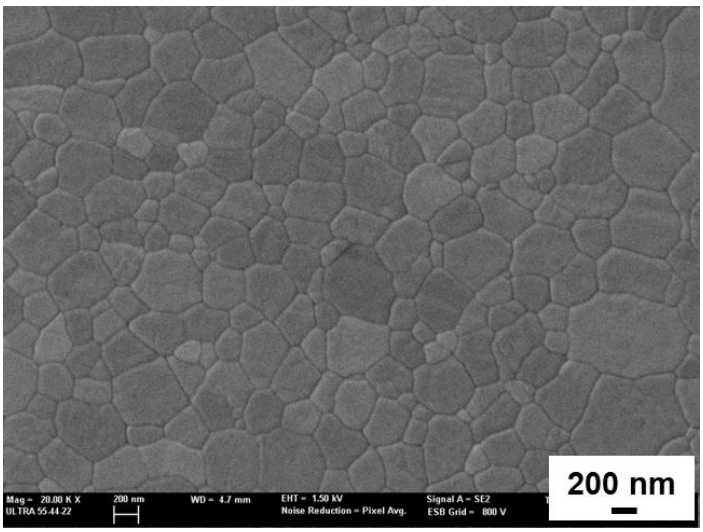

Figure 3. SEM micrographs of the surface of a new ball (up) and the microstructure (down) of the zirconia ceramic balls.

3.2. Polarization curves

The cathodic and anodic polarization curves of the titanium in AS are shown in Figure 4. The initial open circuit potential (E(OCP)) became stable at -0.30 V after one hour of immersion. The logarithm of the cathodic current density during the cathodic polarization (Figure 4 – red dashed line) shows a linear behavior with the applied potential up to -0.6 V. At lower potentials, the relationship between log(|*i*|) and the potential changes due to the mass transport mechanism of the dissolved oxygen reduction and the contribution of water reduction. The anodic polarization scan (black solid line) follows the previous cathodic one, indicating a reversibility of the involved reactions (oxygen and water reduction) on the titanium surface. The average corrosion potential value is E_{corr} = -0.35 V. At potentials above the E_{corr} a first passive plateau is observed between -0.3 and 0.2 V with a passive current density around $i_p \approx 1$ µA/cm^2. Above 0.7 V, current density remains constant at around $i_p \approx 20$ µA/cm^2.

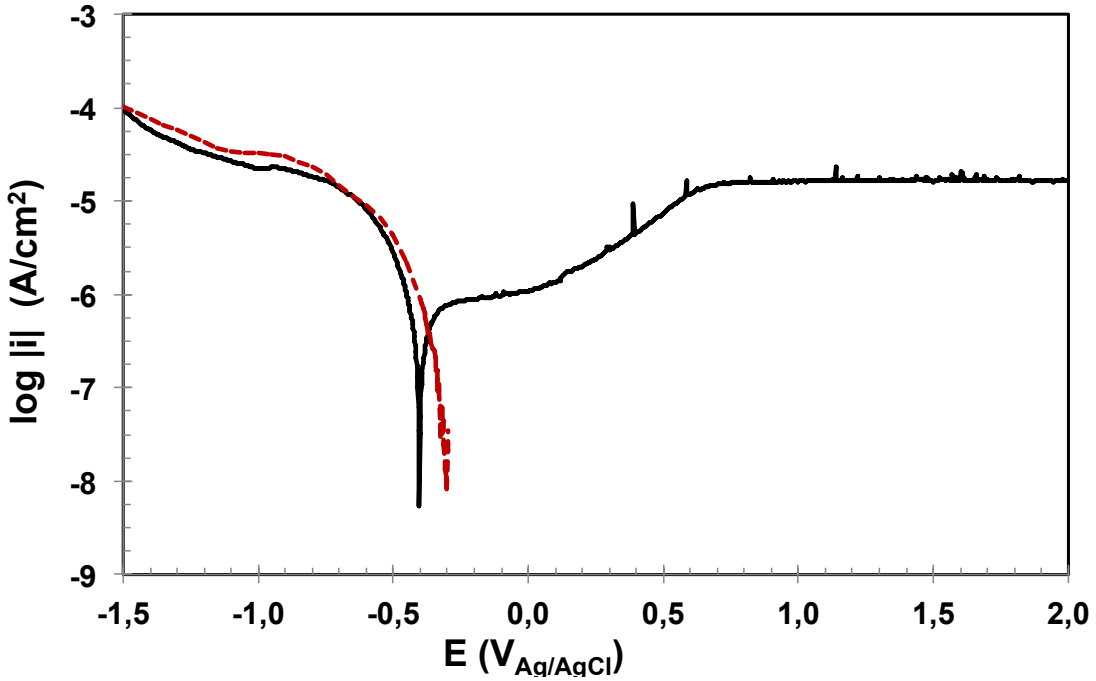

Figure 4. Cathodic (red dashed) and anodic (black solid) potentiodynamic curves of the Ti sample in AS.

The cathodic Tafel coefficients (a_c and b_c), the corrosion potential (E_{corr}) and the passivation current density (i_p) have been extracted from the polarization curves and their values are summarized in Table 4.

Table 4. Electrochemical parameters of the Titanium obtained from the polarization curves.

	Titanium
a_c (V/dec)	-1.18
b_c (V/dec)	0.13
E_{corr} (V)	-0.35
i_p (µA/cm^2)	16.7

3.3. Friction response and electrochemical evolution with time

3.3.1. COF and OCP evolution during sliding

Figure 5 shows the evolution of the OCP of the titanium disk with time during the tribocorrosion tests sliding against a zirconia ball. Prior to rubbing, the OCP was stable around -0.1 V. When rubbing started, potential abruptly decayed due to the mechanical depassivation of the surface and the initial COF value stabilized around 0.45. During the tribocorrosion test, the OCP evolution results from the galvanic coupling established between the depassivated (worn) and still passive (unworn) areas [11]. After the first 300 cycles of rubbing, the OCP of the titanium increased simultaneously to an increase in the COF values. The COF value at the end of the test was 0.74 and the OCP lied around -0.22 V. After rubbing, potential increased towards the initial OCP value due to the final repassivation of the worn surface.

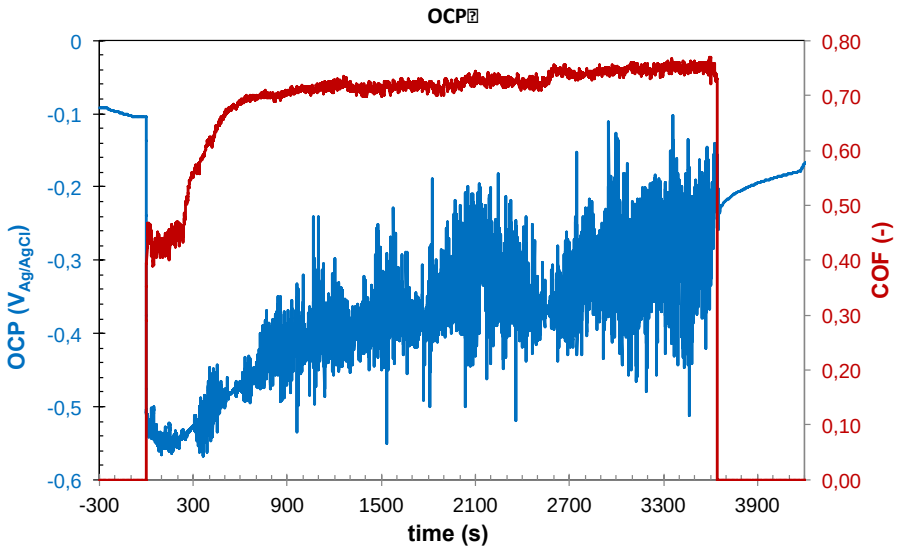

Figure 5. Time evolution of the potential (OCP) and the coefficient of friction (COF) during the tribocorrosion test of the Ti rubbed against ZrO_2 at OCP in AS (F_N = 5 N, ω = 60 rpm, N = 3600 cycles).

3.3.2. Current evolution during sliding

Figure 6a and 6b show the evolution of the measured current and the COF with time during the tribocorrosion test of the titanium sample sliding against the zirconia ball at applied potentials of -1.5 V and 1 V, respectively.

Under cathodic applied potential, Figure 6a, the measured current tended to more negative values during sliding. The COF increased at the onset of rubbing due to the mechanical action of the pin on the Ti surface. The COF exhibited oscillation transients from 0.4 to 0.6 during the tribocorrosion test.

Under anodic applied potential, Figure 6b, an abrupt increase of the current and of the COF were observed at the onset of rubbing. This increase in current is due to the mechanical detachment of the passive film and the consequent depassivation of the titanium surface. The measured current oscillated around a very low value of 15·μA during the tribocorrosion test. The COF followed the current evolution in the opposite direction, progressively increasing during the first 200 seconds of the test and remaining constant around 0.78 during the whole sliding duration. When the sliding

was stopped, the current recovered the value observed at the beginning of the test. These phenomena have been already observed in other studies carried out on titanium alloys [12][13].

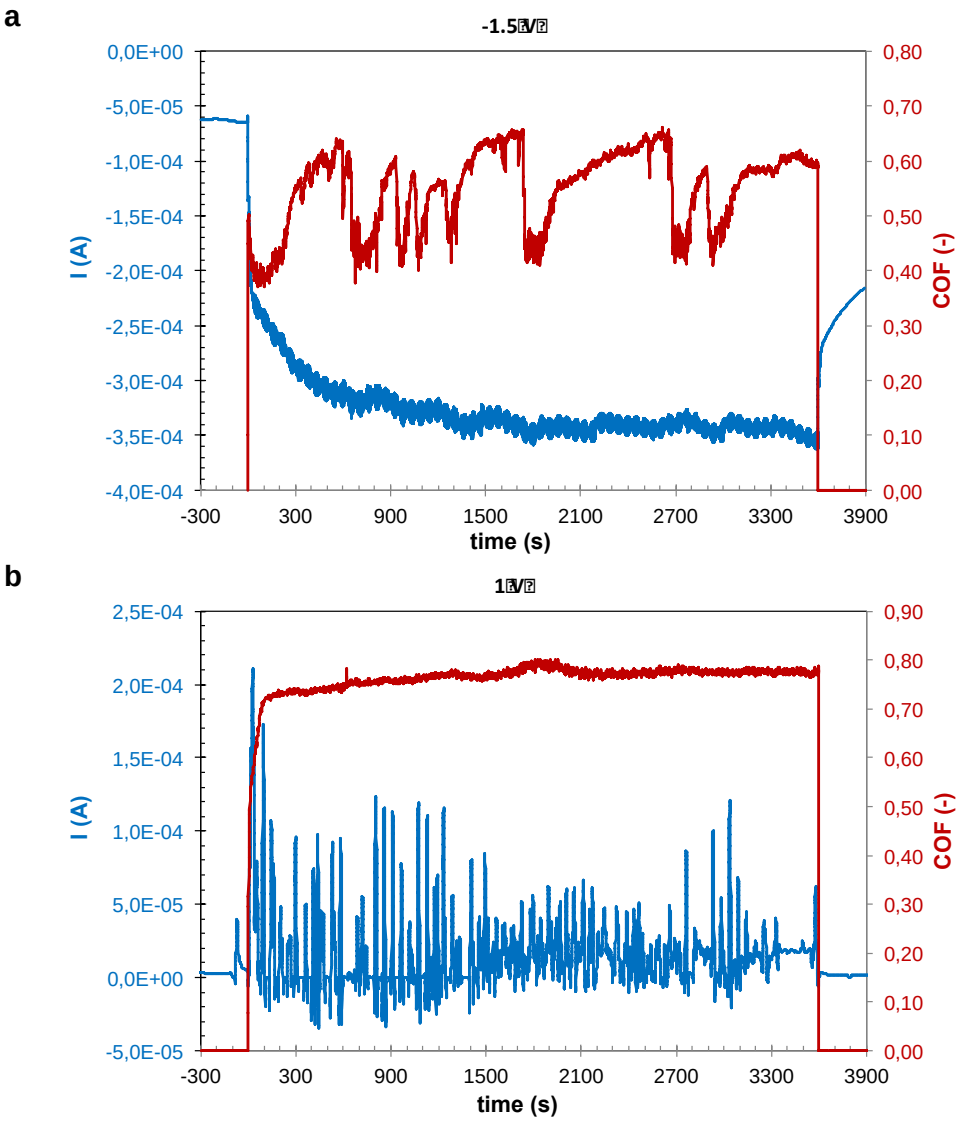

Figure 6. Time evolution of the current (I) and the coefficient of friction (COF) during the tribocorrosion test of the Ti rubbed against ZrO_2 at (a) -1.5 V and (b) 1 V in AS (F_N = 5 N, ω = 60 rpm, N = 3600 cycles).

3.4. Wear quantification

The calculated total wear volumes (V_T), the wear accelerated corrosion volumes (V_{WAC}), the wear track width (w) and the wear coefficients (k) of the titanium disks at different electrochemical conditions are shown in Table 5.

From a mechanistic point of view, the total wear volume (V_T) can be expressed as the sum of the mechanical wear volume (V_{mech}) and the wear accelerated corrosion volume (V_{WAC}) [14]. The latter can be calculated following the Faraday's law using the measured current during the tribocorrosion test and applying equation 1.

$$V_{WAC} = \frac{I_{sliding} M}{nF\rho} \quad (1)$$

Where $I_{sliding}$ is the current during sliding in the tribocorrosion test, t the sliding duration, M the molecular weight of titanium (48 g/mol), n its oxidation state (4), F the Faraday constant (96450 C/mol) and ρ the density of the metal (4.5 g/cm^3).

In the tribocorrosion tests carried out at OCP, the current during sliding can be calculated by applying the galvanic coupling model proposed by Vieira et al. [11]. Thus, the mechanical wear volume can be obtained by the difference between the V_T and the V_{WAC}. At OCP, the V_{WAC} represents the 0.01% of the total wear volume, while at 1 V it is 10% of the total wear volume.

The wear volumes of the Ti samples lie between 15 and 32.5·10^{-3} mm^3, Table 5. At OCP the wear volume is two times lower than at applied potential. The first 300 cycles at OCP condition, the wear volume has already reached the 2/3 of the total wear volume of the test at 3600 cycles.

Table 5. Wear volumes of the titanium samples and the counterparts under different electrochemical conditions

E [V]	N [cycles]	V_T [·10^{-3} mm^3]	k [mm^3/(N·m)]	w [µm]	V_{WAC} [·10^{-3} mm^3]
-0.5 (OCP)	3600	15.24	1.35·10^{-4}	520	3.39·10^{-3}
-0.7 (OCP)	300	10.15	1.08·10^{-3}	525	9.76·10^{-3}
-1.5	3600	31.79	2.81·10^{-4}	730	-
1	3600	32.48	2.87·10^{-4}	625	3.46

The zirconia balls were also analyzed and only some material transfer in the contact area was observed with no wear of the ball. Figure 7a shows an image of the ceramic ball after the tribocorrosion test against the titanium at OCP in AS. The surface profile of the zirconia ball is shown in Figure 7b, where clearly no wear can be observed.

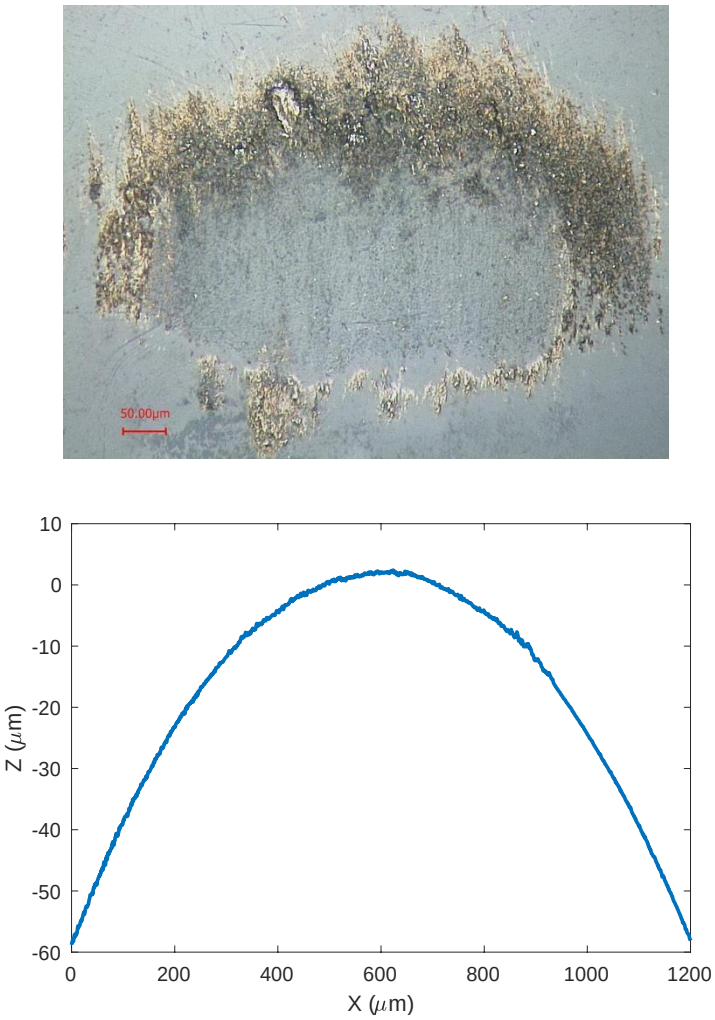

Figure 7. (a) Optical image of the ZrO_2 ball at the end of the tribocorrosion test when rubbed against the titanium during 3600 s at OCP in AS. (b) Surface profile of the zirconia ball.

3.5. Wear morphology

Optical and FESEM images of the wear track at the end of the tribocorrosion tests of the titanium sample sliding against a ZrO_2 ball in AS saliva at different applied potentials and at OCP are shown in Figure 8.

The images illustrate the accumulation and agglomeration of debris leading to the buildup of third bodies as the potential is increased. Under cathodic conditions, at applied potential of -1.5 V, plastic deformation of the titanium surface with very dispersed micrometer size wear debris along the wear track is observed. Under OCP conditions (absence of polarization), the titanium remains passive and, above the deformed titanium surface, accumulated and compacted wear debris is formed. This effect is more pronounced under passive conditions, at an applied passive potential of 1 V, in which extensive formation of a third body layer along the wear track is observed. However, this layer is not continuous and different areas, covered and non-covered by the accumulated wear debris, were found. Under this condition, surface cracks were formed on the smeared wear debris causing its delamination.

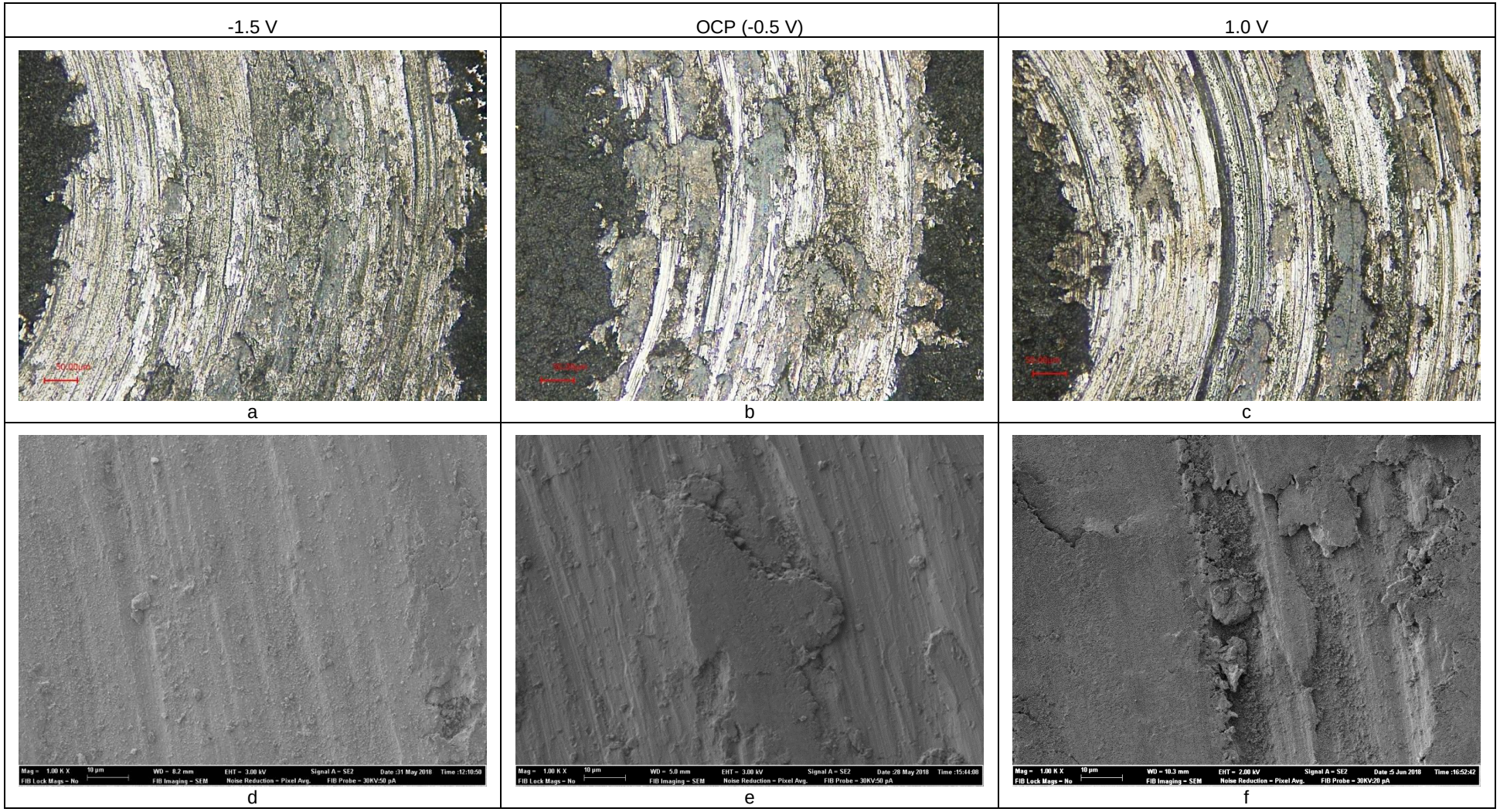

Figure 8. Optical (up) and SEM (down) images of the titanium wear track after 3600 cycles tribocorrosion tests at different applied potentials (a, d) -1.5 V, (c, f) 1 V and (b, e) OCP.

In order to better characterize the wear morphology, FIB cross sections were carried out in the worn area of the titanium tested at OCP. Figure 9 is a SEM image of the worn area with the sites where the FIB cross-sections were carried out indicated with numbers. Figure 10 shows the cross-section corresponding to the site in which compacted debris was formed (point 1 in Figure 9) including an enlargement of the outer part of the profile in Figure 10b. It is possible to observe a thick mixed layer (several micrometers in depth) with presence of cracks perpendicular to the sliding direction. Different areas with more or less oxidized titanium (according to the different brightness in the SEM image) are formed. In the first 500 nm of the cross-section high amount of titanium oxide can be observed mixed with some metallic clusters of material. The cracks are preferentially growing at the interfaces of the different layers but also in the highly deformed titanium. Below the mixed oxide layer, a tribological transformed zone near the worn surface area of the wear track is observed, which is characterized by a grain refinement layer ranging from 3-4 µm in depth. This phenomenon has been already observed and reported by several authors [15][16][17].

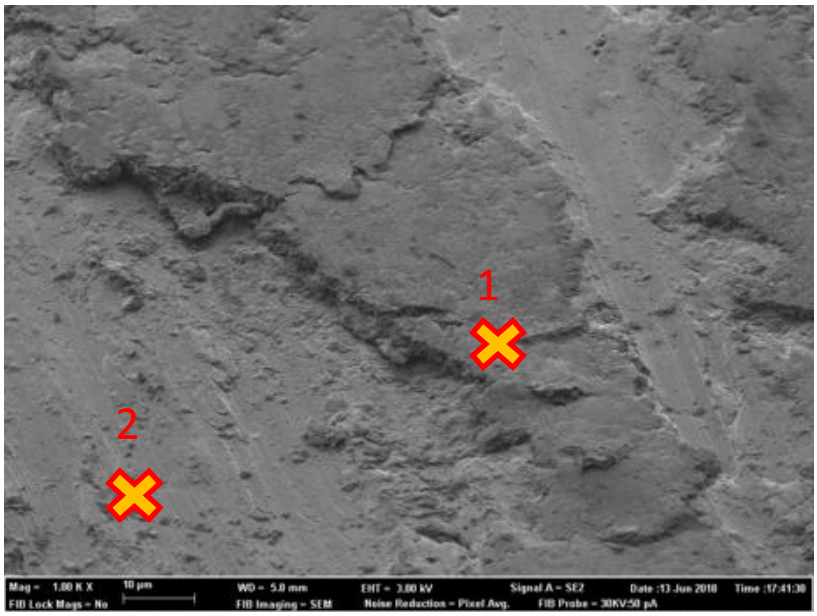

Figure 9. SEM image of the titanium wear track after 3600 cycles of tribocorrosion test at OCP. Numbers show the location of FIB cross-sections in presence (1) and absence (2) of compacted wear debris.

The FIB cross-section at point 2 in Figure 9, where no layer of compacted debris was formed, is shown in Figure 11. In this case, only a grain refinement between 0.5-1 µm in depth is formed and no cracks, neither thick mixed nor smeared layers were observed.

a

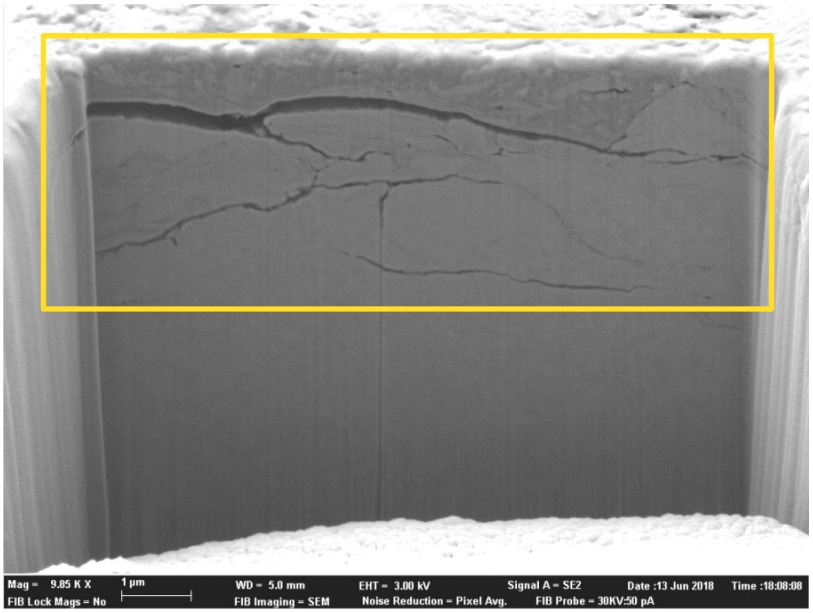

b

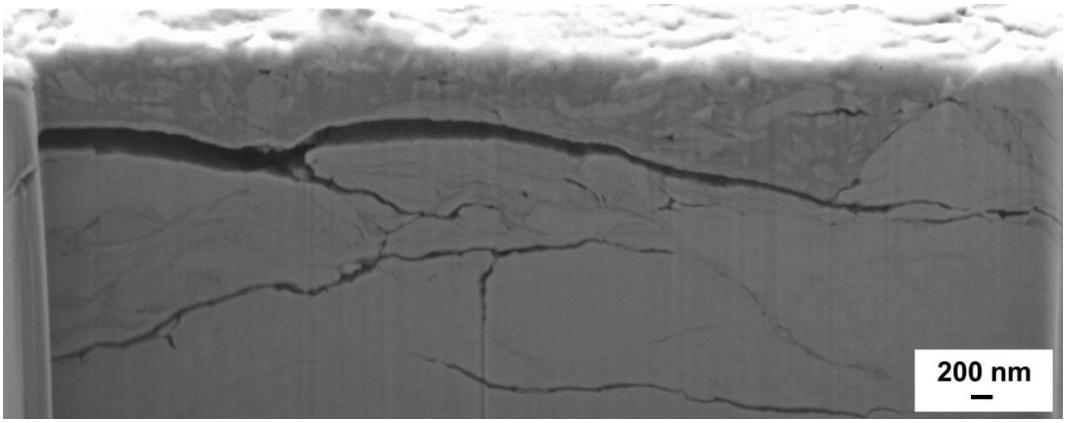

Figure 10. (a) FIB cross-section of the Ti wear track in a section with compacted wear debris. (b) Magnification of the material close to the surface. Point 1 in Figure 9.

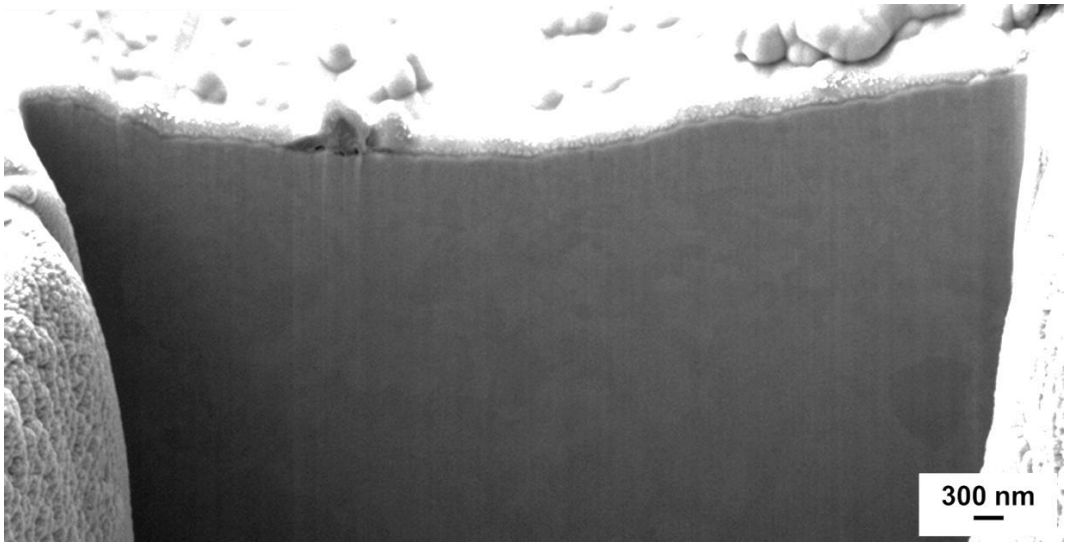

Figure 11. FIB cross-section of the Ti wear track in a section with no compacted wear debris. Point 2 in Figure 9.

4. Discussion

The present results show that the material loss of the tribocorrosion pair Ti/ZrO_2 is influenced by the behavior and the properties of the wear debris formed during the tests which depends on the prevailing electrochemical conditions in the contact. The studied rough titanium surface undergoes severe plastic deformation simultaneously to its oxidation under passive conditions. The deformation of asperities and the mechanical detachment of the passive film under sliding cause the exposure of the underlying metal to the corrosive electrolyte. The surface is then re-oxidized with an oxidation kinetics that depends on the electrode potential [18]. These phenomena occur cyclically, allowing for the continuous exposure of metallic material to be oxidized. The mechanical mixing of metallic titanium and titanium oxide takes place during deformation by burying and smearing surface oxide films and the resulting material accumulates in certain sites of the worn area, Figure 8.

Under cathodic conditions, with a lack of passive film or a very thin one, no chemical wear takes place and the material loss is caused by the mechanical detachment of the plastically deformed asperities. Because the initial roughness of the titanium is very high (around 2.9 μm) the detached wear particles can easily remain between the plastically deformed asperities and they leave the contact during the sliding. The ejection of wear particles may originate the oscillations in the COF observed in Figure 6a. The detached metallic titanium did not adhere on the ceramic ZrO_2 ball, which did not show any mass transfer at the end of the test.

In absence of polarization (tribocorrosion tests at OCP), the titanium surface is passive. The tribocorrosion tests under this condition, Figure 5, show a potential transition during sliding simultaneously to a COF increase after 300 cycles. In order to understand this transition, the same tribocorrosion test at OCP in AS was stopped after 300 cycles and the corresponding wear tracks were analyzed by confocal microscopy (Figure 12a) and SEM (Figure 12b). In these images, an initial state of the material behavior consisting on the deformation of the titanium, mainly at the asperities, and the smearing of oxidized and metallic particles are observed. As the number of cycles increases, the continuous mechanical mixing of metal and oxide particles starts accumulating in certain areas, forming a discontinuous third body along the wear track, Figure 8b and 8e. The sliding takes place then on this formed mixed layer supporting the mechanical loading and reducing wear, Table 5.

a

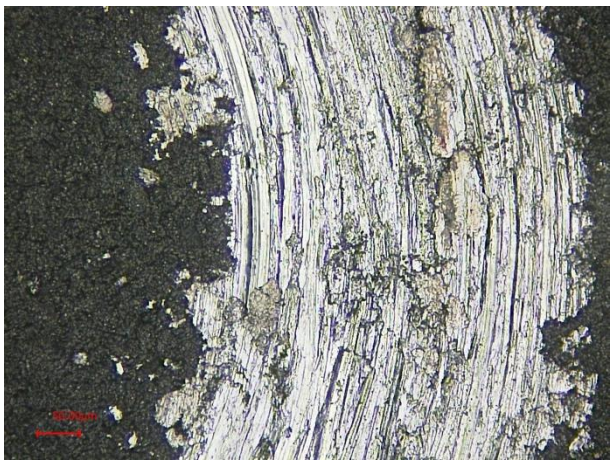

b

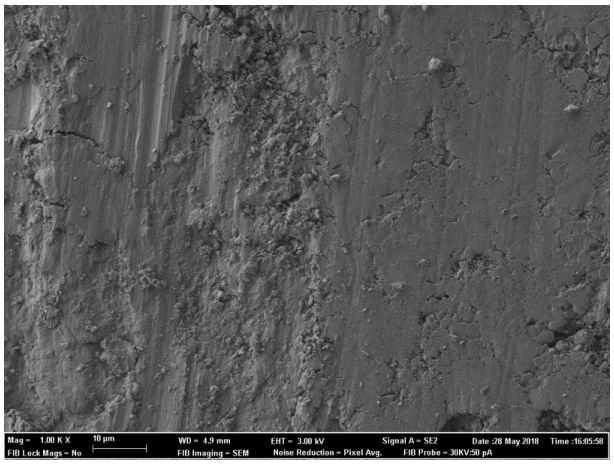

Figure 12. Optical (up) and SEM (down) images of the titanium wear track after 300 cycles of tribocorrosion tests at OCP.

The discontinuity in the third body oxide film is probably caused by its breaking away from the contacting surfaces when a critical thickness is exceeded, leading to the ejection of oxidized wear debris from the contact. This statement is confirmed by the observation that, independently on the tribocorrosion test carried out, the maximum thickness of the compacted layer does not exceed 4 μm. Furthermore, the FIB cross-sections in Figure 10 show the appearance of cracks at the interfaces between the more oxidized and less oxidized areas and the bulk deformed material. This can be attributed to the probably different mechanical properties (hardness and elasticity) of the generated layers, which may cause the stress field at the interface being higher than its strength, thus causing its failure. Cracks are also found deep below the surface, Figure 10, indicating that another acting mechanism, low cycle fatigue, occurs [17]. As a consequence of sufficiently high accumulated stresses (generated by repeated sliding contact) the growth of horizontal subsurface cracks takes place.

These chemo-mechanical phenomena also cause a transfer of material towards the ZrO_2 ball (Figure 13) at the end of the 3600 cycles in the tribocorrosion test, which was not observed before 300 cycles of sliding. The transferred material on the ball corresponded to titanium oxide, which is known to strongly adhere on ceramics [22]. The moment when the sliding starts occurring on the compacted wear debris, and not on the titanium disk surface, can be detected by the simultaneous transition in potential and COF during the tribocorrosion tests at OCP (Figure 5).

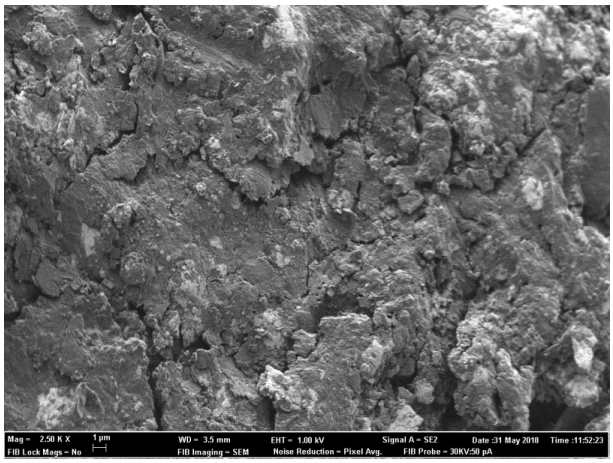

Figure 13. SEM image of the ZrO_2 ball after 3600 cycles of tribocorrosion test at OCP in AS.

It is known that the passivation kinetics and the thickness of the passive film in titanium and titanium alloys depends on the applied potential [19][20][21]. Milosev et al. [19] studied the chemical composition of the passive layer of a Ti20Nb10Zr5Ta titanium alloy in simulated body fluids by XPS analysis at different applied potentials and they observed an increase in the oxide thickness between 2.3 and 4.5 nm/V depending on the electrolyte. Navarro et al. [18] calculated the oxide film thickness in new beta titanium alloys and pure titanium through theoretical models and EIS in sulfuric acid, obtaining similar values and an increase in the oxide film of around 3 nm/V for the pure titanium. Under the studied tribocorrosion conditions, at potentials ranging from -0.3 V to 1 V, a thinner passive layer will be formed at the lowest potential (OCP) and thicker layers as the potential increases (6 nm thicker would be expected at 1 V). Considering that the total plastically deformed area in the contact equals the ratio between the normal force and the hardness of the worn area (F_N / H) and that the thickness of the passive layer at 1 V is around 10 nm, the total amount of oxidized material formed every cycle will be 20 μm^3. This means that twice oxidized material will be generated at 1 V compared to OCP.

It is also under high passive potential, 1 V, that higher wear than the one measured at OCP was observed although the wear morphology is the same under both conditions (plastic deformation and compacted wear debris). Considering that at this potential the passive film is thicker, one can assume that the amount of incorporated oxide to the wear debris is higher. Because the resulting oxidized material is also harder, it causes higher mechanical wear by increasing the contact pressures through the oxide particles.

5. Conclusions

In this work, the tribocorrosion degradation of a titanium/zirconia pair was studied under different electrochemical conditions in AS saliva. From it, the following conclusions can be drawn:

- The total wear volume of titanium and the wear mechanisms when sliding against a zirconia ball depend on the prevailing electrochemical conditions due to their influence on the wear debris properties and behavior. Wear mechanisms change from plastic deformation of asperities in absence of passive layer to third bodies formation in passive conditions. Zirconia does not wear in any case.
- Under cathodic applied potential, when no passive layer or very thin oxide film covers the titanium surface, the wear mechanism is mainly due to the detachment of highly plastic deformed titanium (non or slightly oxidized) with no titanium transfer to the zirconia counterpart.
- The presence of a passive layer on the metal surface allows the formation of a mixed metallic and oxidized compacted layer where the contact takes place. The sliding of the counterpart on this film causes an increase of the coefficient of friction.
- Total wear volume and wear accelerated corrosion increase at high passive potentials. Under these conditions, the amount and the ratio of titanium oxide in the mixed layer is supposed to be higher, thus also higher the final detached material.
- The lowest wear observed at OCP (half the volume than the one measured at cathodic or high passive conditions) is probably a consequence of the properties of the third body and the relation between its formation and its detachment. However, further detailed analysis of the chemical composition of the third body is needed to determine the deformation mechanisms of this layer.

Acknowledgements

Authors would like to acknowledge the Generalitat Valenciana for the financial support under the PROMETEO/2016/040 and GV/2017/042 projects. A. Dalmau acknowledges the Generalitat Valenciana for her contract (APOSTD/2017/051).

References

[1] S. Mischler, Triboelectrochemical techniques and interpretation methods in tribo-corrosion: A comparative evaluation, Tribology International, 41(7) (2008) 573-583. doi: https://doi.org/10.1016/j.triboint.2007.11.003.

[2] S. Mischler, A. Igual Munoz, Tribocorrosion, Encyclopedia of Interfacial Chemistry: Surface science and electrochemistry 1st edition Editor Klaus Wandelt Ed. Elsevier (2018) 504-514.

[3] M. Long, H.J. Rack, Titanium alloys in total joint replacement—a materials science perspective, Biomaterials, 19 (1998) 1621–1639. doi:http://dx.doi.org/10.1016/S0142-9612(97)00146-4.

[4] J.C.M. Souza, M. Henriques, W. Teughels, P. Ponthiaux, J.-P. Celis, L.A. Rocha, Wear and Corrosion Interactions on Titanium in Oral Environment: Literature Review, J. Bio- Tribo-Corrosion, 1 (2015) 13. doi:https://doi.org/10.1007/s40735-015-0013-0.

[5] A. Revathi, A. Dalmau Borrás, A. Igual Muñoz, C. Richard, G. Manivasagam, Degradation mechanisms and future challenges of titanium and its alloys for dental implant applications in oral environment, Mater. Sci. Eng. C., 76 (2017) 1354–1368. doi:https://doi.org/10.1016/j.msec.2017.02.159.

[6] M. Geetha, A.K. Singh, R. Asokamani, A.K. Gogia, Ti based biomaterials, the ultimate choice for orthopaedic implants – A review, Prog. Mater. Sci., 54 (2009) 397–425. doi:http://dx.doi.org/10.1016/j.pmatsci.2008.06.004.

[7] C.L. Sikora, M.F. Alfaro, J.C. Yuan, V.A. Barao, C. Sukotjo, M.T. Mathew, Wear and Corrosion Interactions at the Titanium/Zirconia Interface: Dental Implant Application, J. Prosthodont. 0 (n.d.). doi:https://doi.org/10.1111/jopr.12769.

[8] M.W. Klotz, T.D. Taylor, A.J. Goldberg, Wear at the Titanium-Zirconia Implant-Abutment Interface: A Pilot Study, The International Journal of Oral & Maxillofacial Implants, 26(5) (2011) 970-975

[9] T.A. Mendes, J. Caramês, L.P. Lopes, A.L. Ramalho, Sphere-plane methodology to evaluate the wear of titanium of dental implants: a research proposal, BMC Res Notes, (2018) 11:529. doi:https://doi.org/10.1186/s13104-018-3635-8.

[10] H.M. Grandin, S. Berner, M. Dard, A Review of Titanium Zirconium (TiZr) Alloys for Use in Endosseous Dental Implants, Materials (Basel), 5(8) (2012) 1348–1360. doi:https://doi.org/10.3390/ma5081348.

[11] A.C. Vieira, L.A. Rocha, N. Papageorgiou, S. Mischler, Mechanical and electro-chemical deterioration mechanisms in the tribocorrosion of Al alloys in NaCl and in NaNO3 solutions, Corros. Sci., 54 (2012) 26–35. doi:http://dx.doi.org/10.1016/j.corsci.2011.08.041.

[12] V. Guiñón Pina, A. Dalmau Borrás, F. Devesa, V. Amigó, A. Igual Muñoz, Tribocorrosion behavior of beta titanium biomedical alloys in phosphate buffer saline solution, J. Mech. Behav. Biomed. Mater., 46 (2015) 59–68. doi:https://doi.org/10.1016/j.jmbbm.2015.02.016.

[13] M.P. Licausi, A. Igual Muñoz, V. Amigó Borrás, Tribocorrosion mechanisms of Ti6Al4V biomedical alloys in artificial saliva with different pHs, J. Phys. D-APPLIED Phys., 46 (2013). doi:https://doi.org/10.1088/0022-3727/46/40/404003.

[14] S. Cao, S. Mischler, Modeling tribocorrosion of passive metals – A review, Curr. Opin. Solid State Mater. Sci., (2018).

[15] J. Perret, E. Boehm-Courjault, M. Cantoni, S. Mischler, A. Beaudouin, W. Chitty, J.-P. Vernot, EBSD, SEM and FIB characterisation of subsurface deformation during tribocorrosion of stainless steel in sulphuric acid, Wear, 269 (2010) 383–393. doi:http://dx.doi.org/10.1016/j.wear.2010.04.023.

[16] A. Bidiville, M. Favero, P. Stadelmann, S. Mischler, Effect of surface chemistry on the mechanical response of metals in sliding tribocorrosion systems, Wear, 263 (2007) 207–217. doi:http://dx.doi.org/10.1016/j.wear.2007.01.066.

[17] A. Dalmau, W. Rmili, C. Richard, A. Igual–Muñoz, Tribocorrosion behavior of new martensitic stainless steels in sodium chloride solution, Wear, 368–369 (2016) 146–155. doi:http://dx.doi.org/10.1016/j.wear.2016.09.002.

[18] J. Navarro Laboulais, A. Amigó Mata, V. Amigó Borrás, A. Igual Muñoz, Electrochemical characterization and passivation behaviour of new beta-titanium alloys (Ti35Nb10Ta-xFe), Electrochimica Acta, 227(10) (2017) 410-418. doi:https://doi.org/10.1016/j.electacta.2016.12.125.

[19] I. Milosev, G. Zerjav, J.M. Calderon Moreno, M. Popa, Electrochemical properties, chemical composition and thickness of passive film formed on novel Ti–20Nb–10Zr–5Ta alloy, Electrochimica Acta, 99 (2013) 176–189. doi:https://doi.org/10.1016/j.electacta.2013.03.086.

[20] I. Milosev, T. Kosec, H.-H. Strehblow, XPS and EIS study of the passive film formed on orthopaedic Ti–6Al–7Nb alloy in Hank's physiological solution, Electrochimica Acta, 53 (2008) 3547–3558. doi:https://doi.org/10.1016/j.electacta.2007.12.041.

[21] I. Milosev, M. Metikos-Hukovi, H.-H. Strehblow, Passive film on orthopaedic TiAlV alloy formed in physiological solution investigated by X-ray photoelectron spectroscopy, Biomaterials, 21(20) (2000) 2103-2113. doi:https://doi.org/10.1016/S0142-9612(00)00145-9.

[22] D.H. Buckley, Friction Characteristics in Vacuum of Single Polycrystalline Aluminum Oxide in Contact with Themselves and with Various Metals, In: Jahanmir S, editor. Tribology of Ceramics, Fundamental, Park Ridge: Society of Tribologists and Lubrication Engineers; 1987.